Quantifying the impacts of urban morphology on modifying microclimate conditions in extreme weather conditions

Quantifying the impacts of urban morphology on modifying microclimate conditions in extreme weather conditions

K. Javanroodi[1], V.M. Nik[2], JL. Scartezzini[1]
[1]Ecole Polytechnique Fédérale de Lausanne (EPFL), Lausanne, Switzerland
[2]Lund University, Lund, Sweden
Kavan.javanroodi@epfl.ch, vahid.nik@byggtek.lth.se, jean-louis.scartezzini@epfl.ch

Abstract. It is well-known that the morphology of urban areas modifies the variations of climate variables at microscale; known as microclimate conditions. The complexity of urban morphology can lead to undesired wind conditions or excessive air temperature; particularly in extreme weather conditions. This study attempts to quantify the impacts of urban morphology on the evolution of wind speed and air temperature at the urban canopy layer using Computational Fluid Dynamic (CFD) simulations. In this regard, three urban neighbourhoods are generated based on a novel urban morphology parameterization method and assessed in two extreme low and high wind conditions. Results showed that wind speed (up to 75%) and air temperature (up to 28%) at the microscale can get amplified or dampened in extreme conditions. A negative correlation was observed between wind speed and air temperature variations indicating a great potential to reduce outdoor air temperature through heat removal in urban canyons. The findings of the study are categorized based on the morphological parameters to present a series of design-based strategies for the newly-built urban neighbourhoods.

1. Introduction

According to the UN, about 55% of the world population lives in cities and this number is expected to increase to over 66% by 2050 [1]. The number of cities with a higher than one-million population is projected to increase from 512 in 2016 to over 662 in 2030 [2]. In response to this rapid urbanization, the morphology of cities will change notably due to several massive construction waves; resulting in several interconnected urban neighbourhoods and complex urban morphology. The morphology of an urban area can be defined as urban form (e.g. density, the geometry of buildings, etc.), urban function (e.g. building type, location, etc.), and urban structure (e.g. canyons, open spaces, etc.) [3]. It is widely known that urban morphology can affect the energy performance of buildings [4], and urban comfort [5]. The urban morphology also modifies the variation of climate variables at microscale; known as urban microclimate conditions [6]. The literature in modelling urban morphology to assess the microclimate conditions can be categorized into two main groups of generic and real urban models [7]. To improve the generalizability of the microclimate assessment, developing generic morphologies are suggested based on the most influencing morphological parameters [8]. Several research works have studied the impacts of generic urban morphologies with uniform heights on the variation of wind speed [9] and air/surface temperature [10]. However, to improve the reproducibility of results, it is required to develop more complex urban morphologies to consider height variations, building forms, as well as different architectural layouts, and street canyons [11]. Moreover, further investigation is still required to develop design suggestions for designers to avoid undesired wind speeds and excessive air temperature considering complex urban morphologies [12]. Conditions may worsen by climate change and having stronger and more frequent extreme conditions; particularly in regions characterized by extreme events [13]. This paper aims to address the aforementioned gaps by quantifying the impacts of urban morphology on the evolution of wind speed and air temperature at Urban Canopy Layer (UCL) in extreme wind conditions by the means of

Computational Fluid Dynamic (CFD) simulations. The authors selected Stockholm city in Sweden as the case study. The city is experiencing a dramatically high expansion rate and a construction boom to tackle the rapid population growth challenges, particularly in the districts located at the borderline of the city enclosure. Stockholm has an average air temperature of 3.4 ℃ in cold seasons and 17.5℃ in warm seasons. The average wind speed in January exceeds 3.4 $m.s^{-1}$ and reaches 2.6 $m.s^{-1}$ in June; while hourly near-surface wind speeds exceed 10 $m.s^{-1}$ in cold seasons in non-urban areas (weather station altitude= 43.1 m) [14]. The paper is organized as follows. First, in the methodology section, the adopted techniques and methods to develop the urban morphologies are presented in detail. Then, the settings used for the CFD solver, computational domain, the verification process is described thoroughly. The results are presented in Section 3 including wind speed and air temperature using CFD contours and mean profiles. Moreover, the interactions between wind speed and air temperature are assessed using regression analysis. The major findings of the study are presented in the Conclusion section.

2. Methodology

2.1 Generating the urban morphologies

Three mixed-used dense urban morphologies are generated using a technique namely 'Building Modular Cell' or 'BMC' introduced by Javanroodi et al. [15]. 'BMC' is based on the vertical and horizontal expansion of a basic module ($4\times4\times4m^3$) in an urban setting considering the most influencing morphological parameters. The major morphological parameters considered in this study are Plot Area Ratio (or 'PAR': sum of the floor area of all buildings divided by the total area of the neighbourhood), λ_p (the built area projected onto the ground surface divided by the neighbourhood area), Site coverage index (or 'SC': area of ground floor divided by total area or each sub-site), and Volume Area Ratio (or 'VAR': sum of all building volumes divided by the total area of the neighbourhood). A rectangular site with 184×136m dimensions (total area of 25,024 m^2), two main wide canyons (width=32m), and six narrow canyons (width=8m) is defined as the main platform to develop the urban morphologies based on eighteen distinct H/W ratios. An open green space is considered in the left corner of the neighbourhood (S_{open}=1600m^2, S_{veg}= 576m^2) to represent the vegetation cover index of the selected city. Three architectural layouts are selected out of the most frequent layouts in the study area including compact form (C-form), L-form, and court-yard form (CY) with similar site coverage index (SC=68%, 60%, and 64%). To be able to compare the impact of urban form on the microclimate conditions, a similar height distribution (52 floors in total) with one constant central building (H=48m or 12 floors) is assigned to all three cases. Readers are referred to a previous work of authors [4] for more details on generating the urban morphologies. Figure 1 depicts the process of generating three urban morphologies considering the most influencing morphological parameters.

2.2 Computational domain and CFD solver

The Reynolds-average Navier-Stokes equations (RANS) is adopted for the numerical simulations using the standard k- ε model, as probably the most widely-used turbulence model is used in this study [16]. The main tool for the numerical simulation is Autodesk CFD based on an extensive validation study in an earlier work of the authors [17]. In this validation study, grid sensitivity analysis was carried out with different sizes in Autodesk CFD, comparing to ANSYS Fluent (high-resolution simulation conducted by authors with over 1290537 tetrahedral cells and 2527950 triangular interior faces). Moreover, the results of several similar experiments were compared to validate pressure coefficient and wind speed around the central building of the models [18]. Since this study focuses on both low and high Reynolds numbers, wall function based on the Law of the Wall is used to model turbulent flow near the wall elements; which can provide an opportunity to run several iterations for the urban-scale numerical simulations. Moreover, the Temperature Law of the wall is enforced based on Spalding's Inner Law. A total number of 144 monitor points in sixteen critical locations of each site defined. To calculate the mean wind speed and air temperature profiles at each location, nine monitors points from 2m height above the ground surface to 55m are defined. The convergence of the analysis is tracked using the defined monitor point for each CFD simulation (Figure 1-i).

The computational domain is defined according to standards like AIJ and COST guidelines [19] with 10H from the lateral and behind the model and 20H from its rear (H=48m as the highest building in the

generated cases). Four corresponding wind directions (θ=0, 90, 180, and 270°) are selected to define the computational domain. The inlet-outlet boundary conditions are defined based on these corresponding wind directions (Figure 1-j). Two extreme low (U_{ref}= 0.5 m.s^{-1}) and high (U_{ref}= 7 m.s^{-1}) wind speeds are adopted as inputs at the inlet based on the weather conditions of the selected area. A temperature boundary condition is also defined at the inlet (T_{ref}=30 °C). To count for solar heating, Autodesk CFD solar radiation model is considered based on the input temperature (hereafter referred to as reference temperature) out of mesoscale weather data, True View Factor and solar heating energy balance equation.

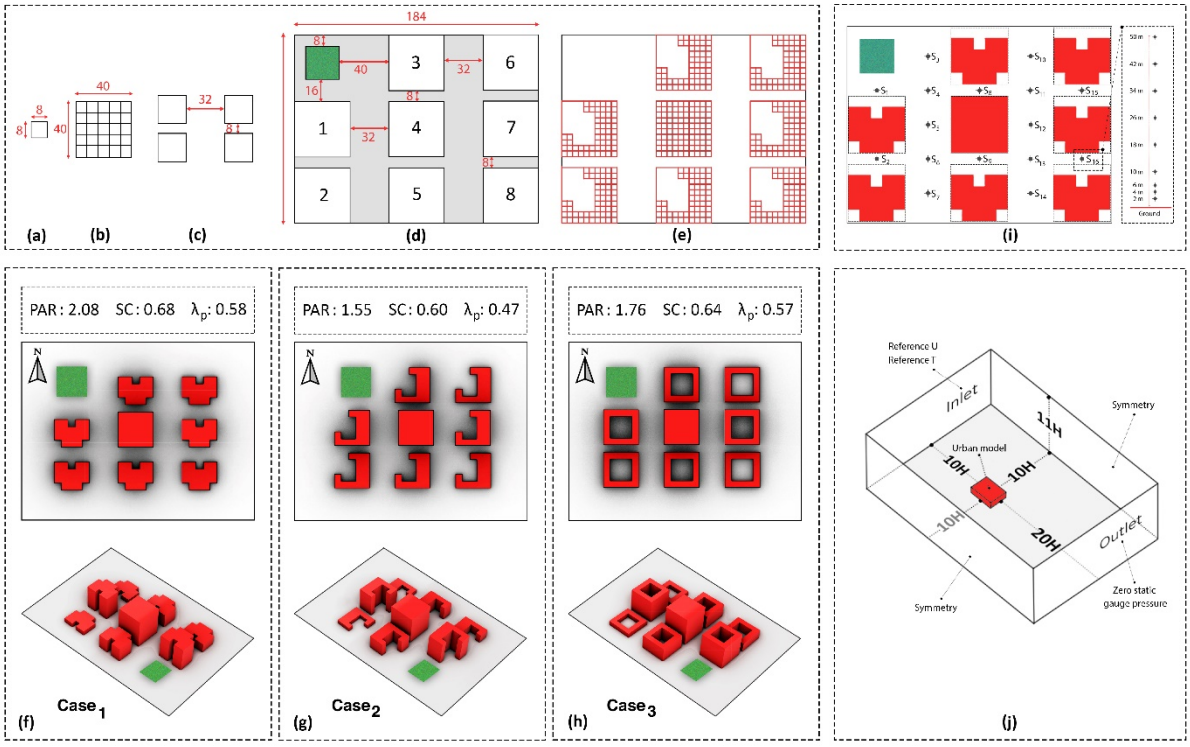

Figure 1: Generated urban morphologies in this study. (a): The basic 4×4×4m^3 module, (b): a sub-site with 10×10 basic modules or 40×40m dimensions, (c): the width of wide and narrow canyons as space between buildings, (d): the urban neighbourhood setting with eight sub-site, and one open green spaces, (e): a sample urban morphology (Case 2) based on defined grids and modules, (f): Case 1, (g): Case 2, and (h): Case 3, (i) defined monitor points at sixteen critical locations of each case and nine monitor points at each critical location are defined to assess the mean wind speed and air temperature profiles (a total number of 144 points for each site), and (j) defined computational domain and boundary conditions in the CFD solver for θ= 270°.

3. Results and discussions

A total number of twenty-four CFD simulations were conducted for the generated cases considering two extreme wind speeds, one extreme warm air temperature and four corresponding wind directions. Figure 2 depicts cross-section wind speed and air temperature CFD contours showing building number 3, 4, 5. A large amount of the wind speed with a corresponding wind direction of θ=0 is blocked by the windward buildings (building 1 with 40m height and building 3 with 24m height) before approaching the entrance of narrow canyons between buildings 4 and 5. Wind speed magnitude with a reference wind direction of θ=180º at the wide canyons is relatively higher compared to θ=0º. The reason is the channelling effect at the eastern street (H/W=1.5 at the entrance with θ=180º) amplifies the wind speed at the near ground surfaces compared to the wind direction of θ=0. In θ=90º, the windward buildings are facing back toward the approaching wind flow; which directs the wind flow toward the windward canyons (narrow canyons between buildings 6,7, and 8). Similarly, in θ=270º the flow is trapped in the windward canyons (narrow canyons between buildings 1 and 2). For example, in Case 3, the wind flow is directed toward the courtyard of the building 1 and 2 and does not reach the wide canyons. A closer look into the air temperature contours in the narrow canyons shows considerably lower temperature in the windward canyons. For example, in Case 3 with the θ=90º, the air

temperature at 2m to 18m surfaces is notably higher in eastern canyons (narrow canyons between building 6, 7, 8) compared to western ones (narrow canyons between building 1, 2, 3).

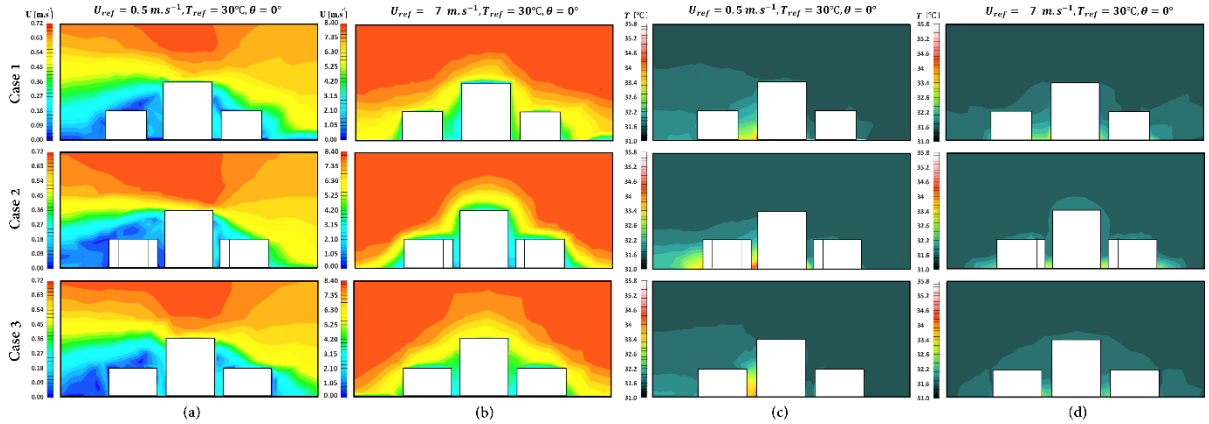

Figure 2. Vertical slices intersecting central buildings of each case (buildings number 3, 4, 5) displaying a colour contour of wind speed (a, b) and air temperature (c, d) with θ = 270°, and T_{ref}=30 °C: (a), and (c) extreme low wind speed of U_{ref}=0.5m.s^{-1}; (b) and (d) extreme high wind speed of U_{ref}=0.5m.s^{-1}

To further assess the impacts of urban morphology on the variations of microclimate conditions, the mean wind speed and air temperature profiles are analysed (Figure 3). An overview of the mean wind speed profiles indicates similar distributions in the considered reference wind speeds. For example, in θ=270º the standard deviation difference between lowest and highest monitor points in the narrow canyons is 45% for Case 1 and 41% for Case 2 with U_{ref}=0.5 m.s^{-1} scenario; while with U_{ref}=7 m.s^{-1} scenario this number is about 35% for both cases. In θ=180º, the average and absolute wind speed interestingly coincide in all three cases, while in other reference wind directions the wind speed varies between cases. The highest absolute wind speed at 2m levels occurred in Case 2 in θ=0, 90, 180º, while in θ=270º this number is seen in Case 3. The highest difference between the bottom and the top of narrow canyons in θ=0, and 90º occurs in Case 1; while in θ=180, and 270º is seen in Case 3 and Case 2 respectively. The normalized mean temperature profiles are affected by the urban morphology and reference wind speed. Overall, air temperature at the near ground surface is about 3.9 to 5.1°C higher than the reference air temperature. The average air temperature at the microscale with U_{ref}=0.5, and 7 m.s^{-1} shows 1 to 2.1 °C temperature difference as an impact of higher heat removal with higher mesoscale wind speeds. For example, in θ=90, 180 and 270º Case 2 shows 0.6, 1.1, and 1.3°C lower temperature with a higher reference wind speed.

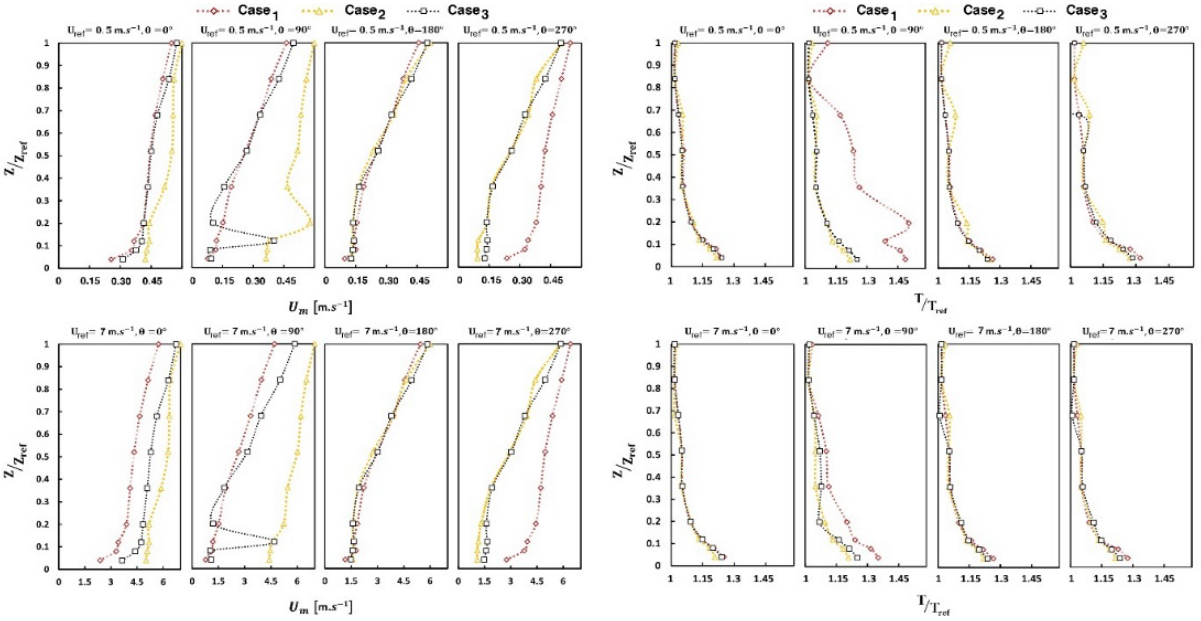

Figure 3. Mean wind speed (right panel), and air temperature (left panel) for all three cases with reference extreme low (0.5 m.s^{-1}) and high (7 m.s^{-1}) wind speeds, T_{ref}=30 °C, and four corresponding wind directions.

Scatterplots of normalized wind speed as a function of normalized air temperature with the best-fitting lines out of all monitor points are presented in Figure 4. A significant correlation between wind speed and air temperature is noticed in Case 3 in all wind directions. In the case of U_{ref}=0.5 m.s^{-1}, the coefficient of determination between wind speed and air temperature variations is 0.68, 0.98, 0.91, and 0.82 for θ=0, 90, 180 and 270º. A similar condition can be seen for Case 2, whereas a coefficient of determination of 0.86, 0.92, and 0.84 is seen for θ=0, 90, and180º; while in θ= 270º under the impact of open space the flow gets more complex and the coefficient of determination falls to 0.57. In the case of U_{ref}=7 m.s^{-1}, a notable lower correlation can be seen in all three cases. The strongest correlation in Case 3 is observed in θ=90, and 270º with R^2 of 0.87 and 0.95 respectively, where approaching flow is perpendicular to the wide canyons. This is while for Case 1 and 2 with more complex building forms, the coefficient of determination is lower than 0.79 in all wind directions. This can indicate the importance of urban morphology in extreme wind speed in causing undesired winds and higher air temperature.

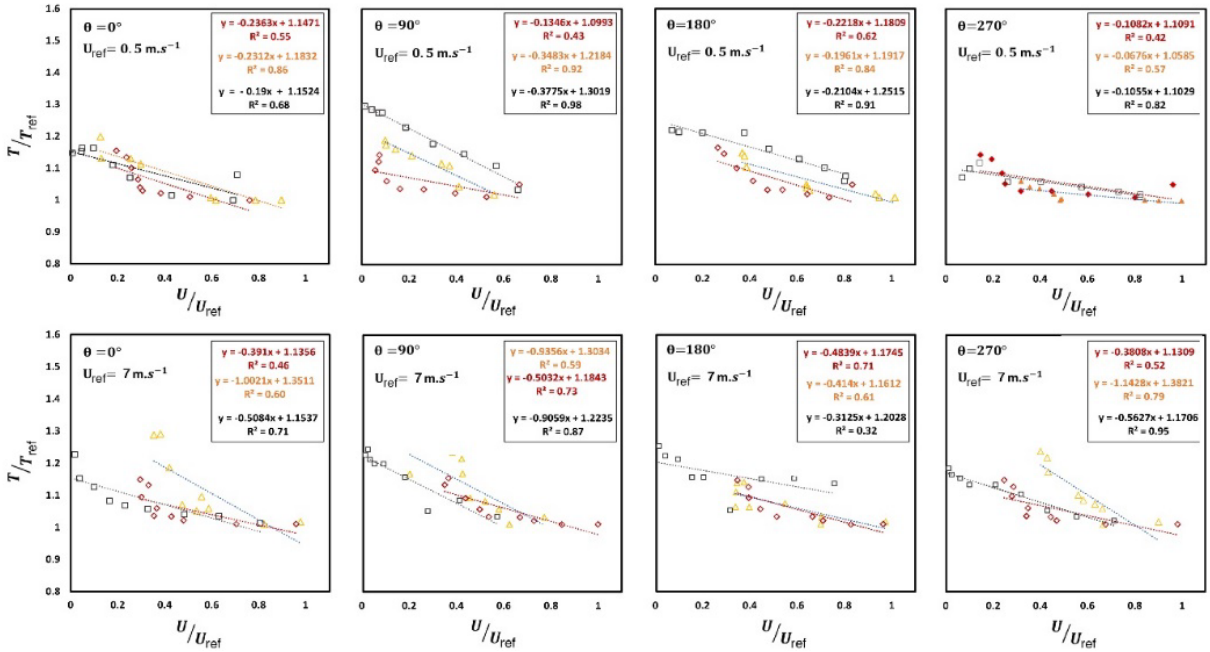

Figure 4. Linear regression between normalized wind speed and air temperature for U_{ref}=0.5 m.s^{-1} (top panel) and U_{ref}=7 m.s^{-1} (bottom panel)

4. Conclusions

This study provided more evidence on the importance of considering variations of climatic variables in urban-scale studies. Results showed the impact of urban morphology on the microclimate conditions by amplifying or dampening the variations of wind speed (up to 75%) and air temperature (up to 28%) from top to the bottom of urban canopy layer. These impacts can be critical to study urban comfort at the pedestrian level and controlling natural ventilation through the building's cluster at the early stage of design. As the limitation of the present study, the urban cases developed cannot represent all complexities of a real urban area. Further investigation is required to quantify wind speed and air temperature fluctuations in different urban settings. The major findings of this study are as the following:

- Dense urban area with C-form buildings showed the highest average air temperature and lowest average wind speed magnitudes in all corresponding wind directions in both extreme low and high speeds compared to other cases.
- A significant negative correlation was observed between the interactions of wind speed and air temperature in urban areas with courtyard buildings in the extreme low wind speeds.
- The highest standard deviation difference of wind speed at urban canopy layer was observed at the narrow canyons compared to the wide canyons.

- In the reference wind direction of θ=0 and 270º with similar windward building height, a direct relation between built density and standard deviation variations was noticed; where higher density results in higher standard deviation magnitudes.
- In extreme high wind speeds, lower average air temperature was observed in the narrow canyons compared to wide canyons due to higher wind speed insde the narrow canyons and the impacts of shading.
- Flow in the windward narrow canyons can be variated up to 23% on average compared to wide canyons; whereas in the windward wide canyons a large amount of flow is directed toward higher elevations.

References

[1] Brockerhoff M, Nations U. World Urbanization Prospects: The 2018 Revision. Population and Development Review 2018;24:883. https://doi.org/10.2307/2808041.
[2] World Urbanization Prospects - Population Division - United Nations-2014 Revision. NewYork: n.d.
[3] Javanroodi K. Wind-phil Architecture: Optimization of high-rise buildings form for efficient summer cooling in Tehran. Tarbiat Modares University, 2018.
[4] Perera ATD, Javanroodi K, Nik VM. Climate resilient interconnected infrastructure: Co-optimization of energy systems and urban morphology. Applied Energy 2021;285. https://doi.org/10.1016/j.apenergy.2020.116430.
[5] He B-J, Ding L, Prasad D. Relationships among local-scale urban morphology, urban ventilation, urban heat island and outdoor thermal comfort under sea breeze influence. Sustainable Cities and Society 2020;60:102289. https://doi.org/10.1016/j.scs.2020.102289.
[6] Oke TR. Urban Climates. 1st edition. Cambridge: Cambridge University Press; 2017.
[7] Bherwani H, Singh A, Kumar R. Assessment methods of urban microclimate and its parameters: A critical review to take the research from lab to land. Urban Climate 2020;34:100690. https://doi.org/10.1016/j.uclim.2020.100690.
[8] Apreda C, Reder A, Mercogliano P. Urban morphology parameterization for assessing the effects of housing blocks layouts on air temperature in the Euro-Mediterranean context. Energy and Buildings 2020;223:110171. https://doi.org/10.1016/j.enbuild.2020.110171.
[9] Allegrini J, Dorer V, Carmeliet J. Influence of morphologies on the microclimate in urban neighbourhoods. Journal of Wind Engineering and Industrial Aerodynamics 2015;144:108–17. https://doi.org/10.1016/j.jweia.2015.03.024.
[10] Chen H-C, Han Q, De Vries B. Modeling the spatial relation between urban morphology, land surface temperature and urban energy demand. Sustainable Cities and Society 2020;60:102246. https://doi.org/10.1016/j.scs.2020.102246.
[11] Javanroodi K, Nik VM. Interactions between extreme climate and urban morphology: Investigating the evolution of extreme wind speeds from mesoscale to microscale. Urban Climate 2020;31:100544. https://doi.org/10.1016/j.uclim.2019.100544.
[12] Bouketta S, Bouchahm Y. Numerical evaluation of urban geometry's control of wind movements in outdoor spaces during winter period. Case of Mediterranean climate. Renewable Energy 2020;146:1062–9. https://doi.org/10.1016/j.renene.2019.07.012.
[13] Nik VM. Making energy simulation easier for future climate – Synthesizing typical and extreme weather data sets out of regional climate models (RCMs). Applied Energy 2016;177:204–26. https://doi.org/10.1016/j.apenergy.2016.05.107.
[14] Start | SMHI n.d. https://www.smhi.se/en/q/Stockholm/2673730 (accessed June 23, 2021).
[15] Javanroodi K, Mahdavinejad M, Nik VM. Impacts of urban morphology on reducing cooling load and increasing ventilation potential in hot-arid climate. Applied Energy 2018;231:714–46. https://doi.org/10.1016/j.apenergy.2018.09.116.
[16] Al-Sallal KA, Al-Rais L. Outdoor airflow analysis and potential for passive cooling in the traditional urban context of Dubai. Renewable Energy 2011;36:2494–501. https://doi.org/10.1016/j.renene.2011.01.035.
[17] Javanroodi K, Mahdavinejad M, Nik VM. Impacts of urban morphology on reducing cooling load and increasing ventilation potential in hot-arid climate. Applied Energy 2018;231:714–46. https://doi.org/10.1016/j.apenergy.2018.09.116.
[18] Javanroodi K, Nik VM. Impacts of Microclimate Conditions on the Energy Performance of Buildings in Urban Areas. Buildings 2019;9:189. https://doi.org/10.3390/buildings9080189.
[19] Tominaga Y, Mochida A, Yoshie R, Kataoka H, Nozu T, Yoshikawa M, et al. AIJ guidelines for practical applications of CFD to pedestrian wind environment around buildings. Journal of Wind Engineering and Industrial Aerodynamics 2008;96:1749–61. https://doi.org/10.1016/j.jweia.2008.02.058.